Electronic Supplementary Material (ESI) for Nanoscale.

Supporting Information

Synergistic ligand exchange and UV curing of PbS quantum dots for effective surface passivation

Hadi Tavakoli Dastjerdi,[1] Daniel Prochowicz,[2] Pankaj Yadav,[3] and Mohammad Mahdi Tavakoli[4*]*

[1]*Department of Materials Science and Engineering, Massachusetts Institute of Technology, Cambridge, MA 02139, USA*

[2]*Institute of Physical Chemistry, Polish Academy of Sciences, Kasprzaka 44/52, 01-224 Warsaw, Poland*

[3]*Department of Solar Energy, School of Technology, Pandit Deendayal Petroleum University, Gandhinagar-382 007, Gujarat, India*

[4]*Department of Electrical Engineering and Computer Science, Massachusetts Institute of Technology, Cambridge, MA 02139, USA*

E-mails: haditavakoli.nano@gmail.com, hadit@mit.edu
mtavakol@mit.edu

Table S1. PV performance of reference and UV-treated PbS QDs devices

PV characteristics of reference and UV-treated PbS QDs devices under 100 mW cm^{-2} AM1.5G illumination. Mean and standard deviations are calculated for six devices in each sample.

Device	V_{OC} (mV)	J_{SC} (mA/cm^2)	FF	PCE (%)
As-prepared	609±5	27.4±0.2	0.54±03	9.0±0.3
30 s-UV-exposed	617±6	28.6±0.1	0.56±0.04	9.9±0.3

60 s-UV-exposed	632±3	28.7±0.1	0.59±0.03	10.7±0.2
150 s-UV-exposed	612±6	28.1±0.1	0.56±0.05	9.6±0.3

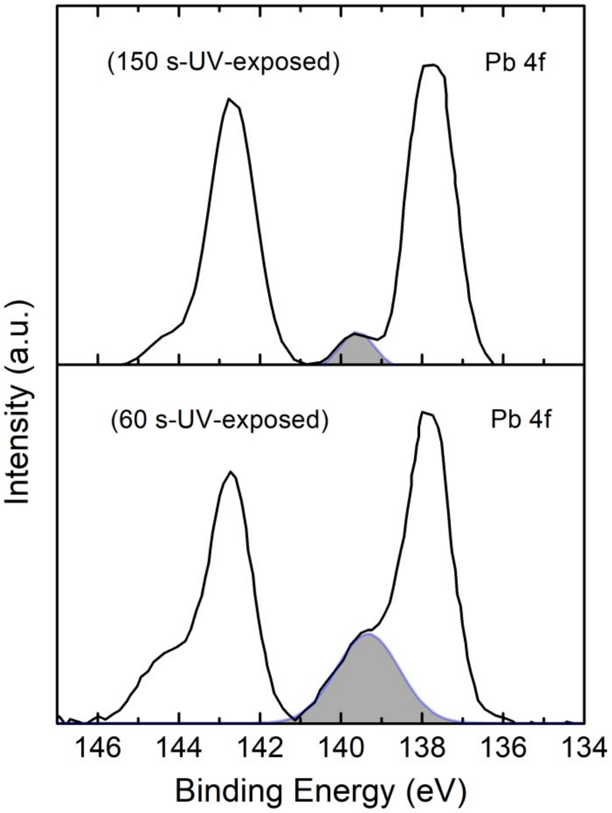

Fig. S1. Pb 4f XPS spectra of the optimized UV-treated (60 sec) and 150 sec UV-treated PbS QDs exchanged with TBAI.

Note. 1

The doping concentrations for PbS-TBAI and PbS-EDT films with and without UV treatment were calculated from capacitance –voltage measurements using the slope of $1/C^2$-V Mott-Schottky plots and the following equation:

$$\frac{1}{C^2} = \frac{2}{qNA^2\varepsilon_0\varepsilon_r}(V - V_{bi} - \frac{KT}{q})$$

Where, C is the capacitance of depletion region, q is the elementary charge, N is the doping concentration, A is the area, ε_0 is the permittivity of vacuum, ε_r is the dielectric constant of the PbS QDs (17.5 for PbS-EDT and 18 for PbS-TBAI) [S1], k is the Boltzmann's constant, T is the temperature, V_{bi} is the built-in potential and V is the applied potential.

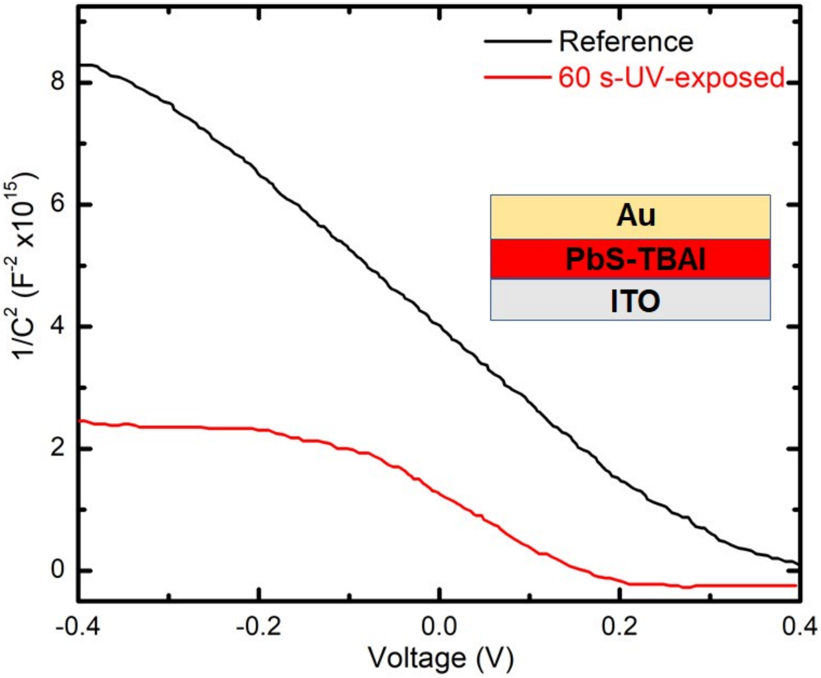

Fig. S2. Mott-Schottky plots, for reference and UV-treated PbS-TBAI QDs.

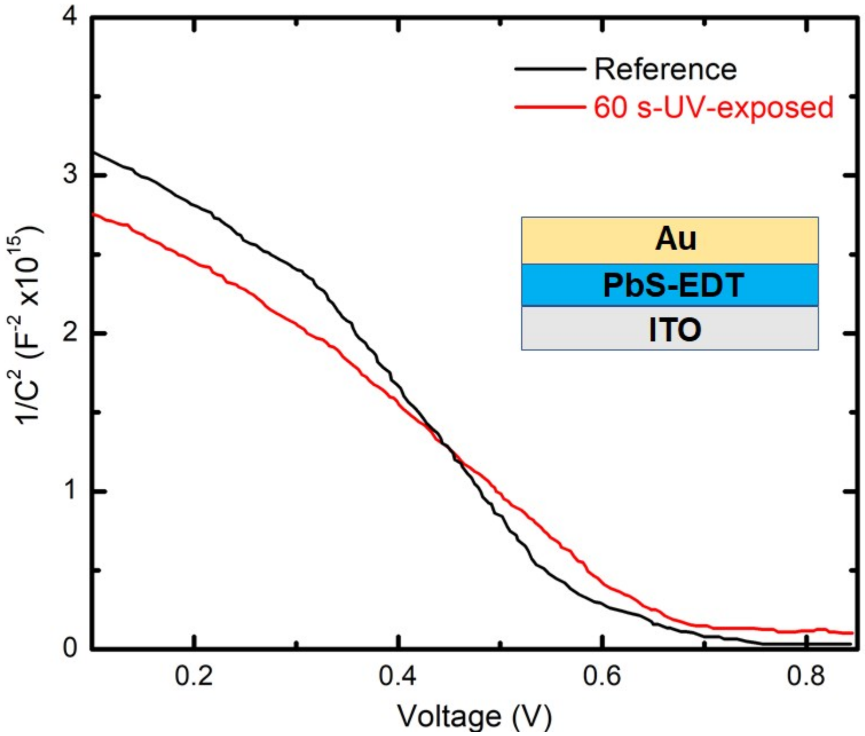

Fig. S3. Mott-Schottky plots, for reference and UV-treated PbS-EDT QDs.

Table S2. Doping concentrations of PbS-TBAI and PbS-EDT films with and without UV treatment

Film	Doping concentration (cm^{-3})
PbS-TBAI (reference)	1.96×10^{17}
PbS-TBAI (UV-treated)	3.12×10^{17}
PbS-EDT (reference)	3.07×10^{17}
PbS-EDT (UV-treated)	4.42×10^{17}

Table S3. Series and shunt resistances of reference and UV-treated PbS QDs PVs

Series and shunt resistances of reference and UV-treated Pbs QDs devices, extracted from dark current measurements

Device	**R_{sh} (Shunt resistance)** **(KΩ/cm^2)**	**R_S (Series resistance)** **(Ω/cm^2)**
Reference	3.03±0.04	7.1±0.2
UV-treated	4.82±0.09	2.8±0.1

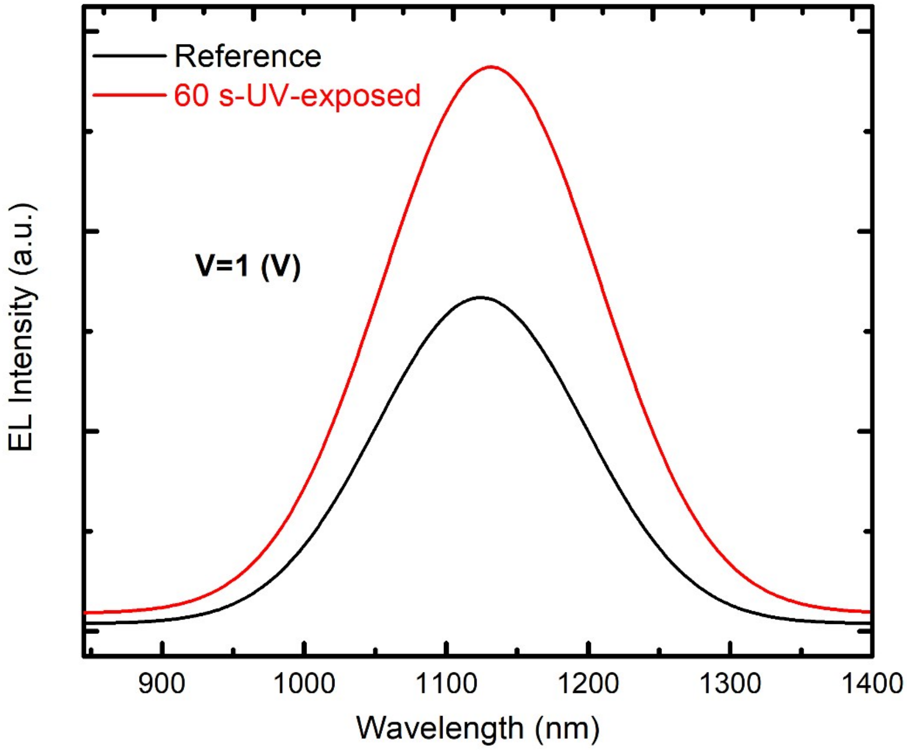

Fig. S4. Electroluminescence spectra. Measured electroluminescence spectra for reference and UV-treated devices. The measurements were done under V=1 (0) bias.

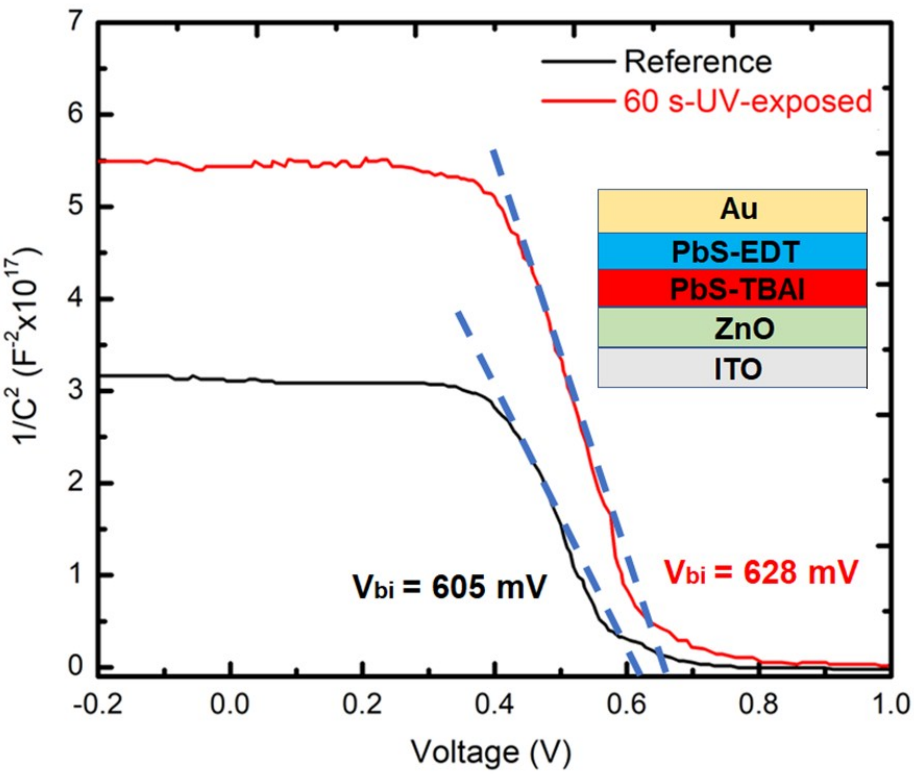

Fig. S5. Capacitance-voltage measurements for the built-in potential of reference and UV-treated PbS QDs devices.

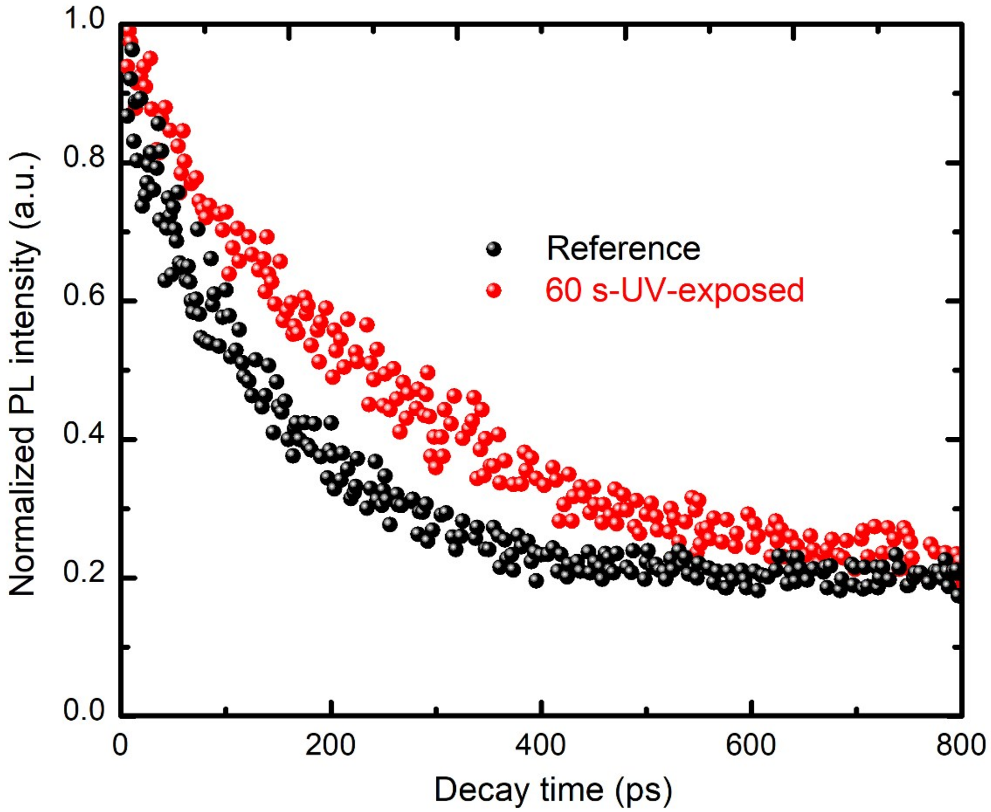

Fig. S6. TRPL measurements. TRPL decay of EDT-exchanged PbS QDs films with and without UV treatment (See Table S4).

Note. 2

UPS measurements of the PbS-TBAI and PbS-EDT with and without UV exposure are shown in Supplementary Fig. 6 and 7. The intersection of the linear part of the spectra near the low binding energy region with the baseline is equal to the difference between the Fermi level and valence band maximum. Also, the Fermi level is equal to the difference between the work function and the vacuum level. The work function is equal to the difference between the incident photon energy (21.2 eV) and the binding energy of the secondary electron cut-off. Therefore, the UPS measurement results were used to extract Fermi and valence band maximum energy levels. The conduction bands were then calculated using the corresponding band gaps and valence band maxima. Using the extracted parameters from UPS measurements, the energy band diagrams of the devices fabricated with and without UV exposure were calculated and plotted in Supplementary Fig. S9 and Fig. S10.

Upon UV treatment, the conduction band of PbS-TBAI shifts from -4.24 eV to -4.28 eV which is closer to the conduction band level of ZnO ETL layer (i.e. -4.3 eV). This facilitates the electron transport from absorber layer to ETL. Also, the down-shift of the Fermi level of UV-treated PbS-

EDT film brings it closer to the work function of Au (~ -5.1 eV) and therefore facilitates hole transfer to the anode electrode which explains reduced series resistance of the UV-treated device shown in Supplementary Table 3 and its overall PV enhancement. Moreover, the difference in conduction band of UV-treated PbS-TBAI and PbS-EDT layers increase to 0.63 eV compared to 0.57 eV for the reference films and leads to improved electron blocking impact of the PbS-EDT layer.

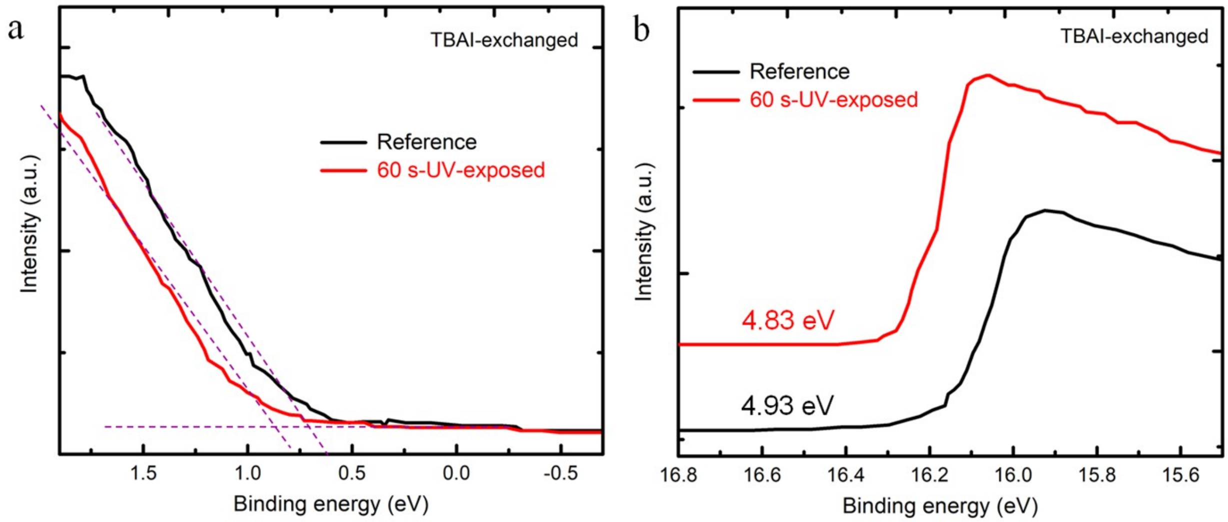

Fig. S7. UPS characterization. a) Magnified UPS spectra near the Fermi edge and b) UPS secondary electron cut-offs of the TBAI-exchanged PbS QDs films with and without UV-treatment. The measured Fermi levels with respect to vacuum level are shown for each film.

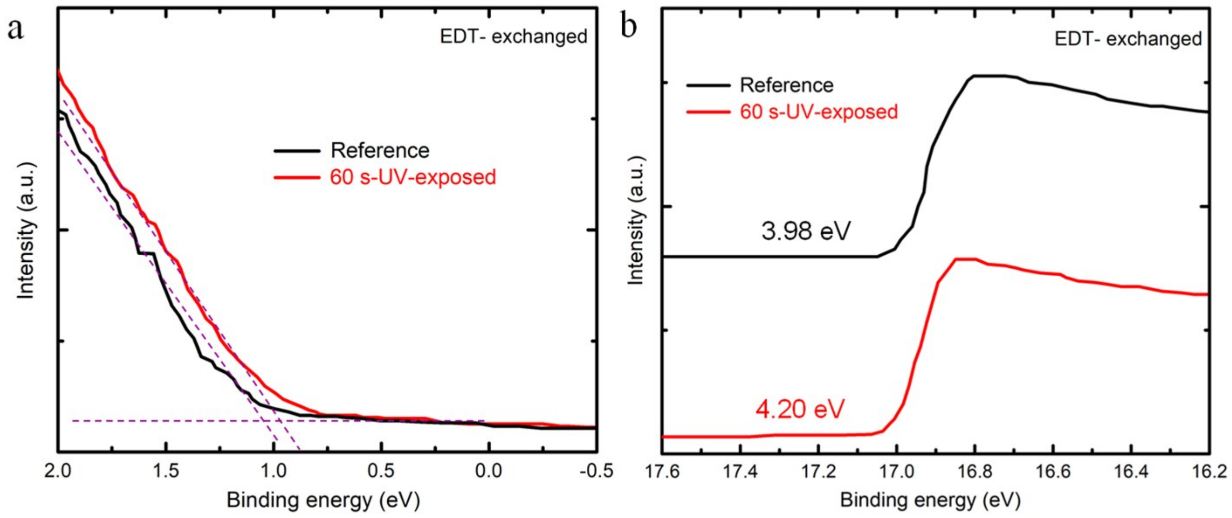

Fig. S8. UPS characterization. a) Magnified UPS spectra near the Fermi edge and b) UPS secondary electron cut-offs of the EDT-exchanged PbS QDs films with and without UV-treatment. The measured Fermi levels with respect to vacuum level are shown for each film.

Table S4. TRPL measurement data

Fitting parameters of the TRPL measurements for PbS-TBAI and PbS EDT with and without UV treatment

Film	A	τ (ps)
PbS QDs-TBAI (reference)	0.91	149
PbS QDs-TBAI (UV-treated)	0.93	288
PbS QDs-EDT (reference)	0.92	136
PbS QDs-EDT (UV-treated)	0.89	245

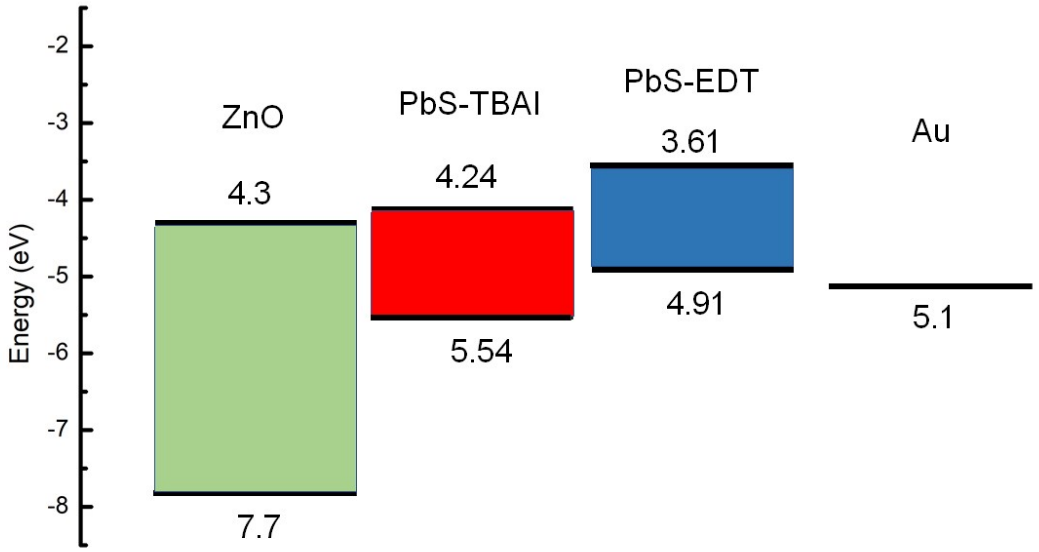

Fig. S9. The energy level diagram of the reference PbS QD solar cell with reference to the vacuum level, plotted from the UPS results shown in Fig. S7 and Fig. S8.

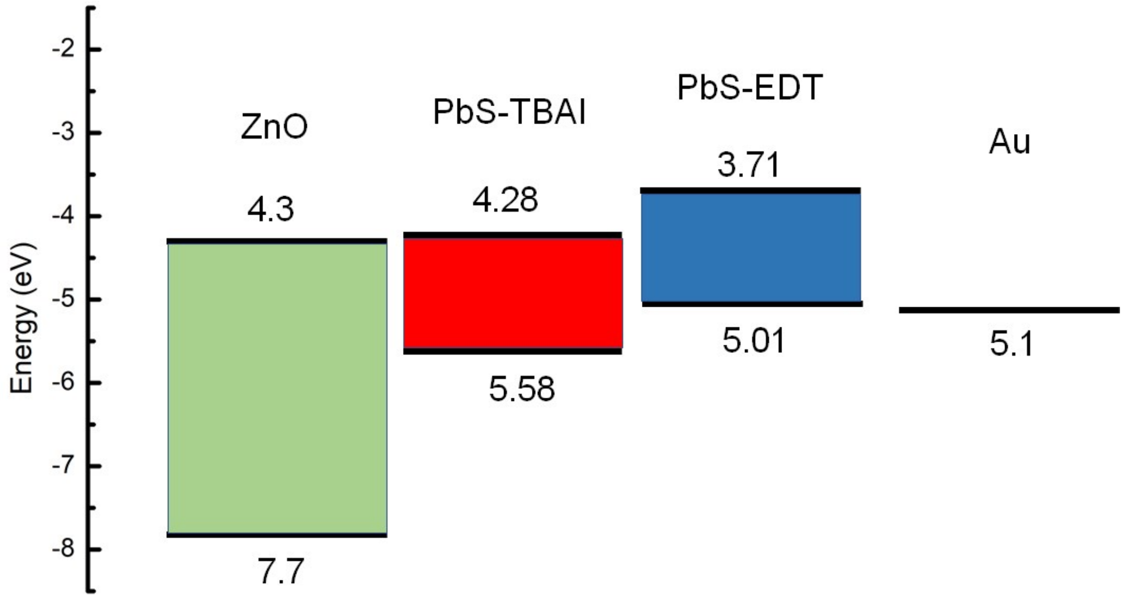

Fig. S10. The energy level diagram of the UV-treated PbS QD solar cell with reference to the vacuum level, plotted from the UPS results shown in Fig. S7 and Fig. S8.

References:

[S1] M. J. Speirs, D. N. Dirin, M. Abdu-Aguye, D. M. Balazs, M. V. Kovalenko, M. A. Loi, *Energy Environ. Sci.* 2016, **9**, 2916-2924.